RSC Advances

ROYAL SOCIETY OF CHEMISTRY

www.rsc.org/advances

RSC Advances

RSCPublishing

ARTICLE

Oleic acid assisted formation mechanism of $CuInS_2$ nanocrystals with tunable structures

Cite this: DOI: 10.1039/x0xx00000x

Fengcong Gong, Shouqin Tian*, Baoshun Liu, Dehua Xiong, Xiujian Zhao*

Received 00th April 2014,
Accepted 00th May 2014

DOI: 10.1039/x0xx00000x

www.rsc.org/

Abstract: Distinct from the popular opinion that the only zincblende $CuInS_2$ phase could be prepared at the presence of oleic acid (OA), $CuInS_2$ nanocrystals with different phase structures and shapes were synthesized by a facile heat-up method through simply adjusting the OA dosage. Zincblende $CuInS_2$ quantum dots (QDs) with a triangular pyramid shape were obtained at a low dosage of OA (< 1 mL). With an increase in the OA dosage (~1.5 mL), wurtzite $CuInS_2$ hexagonal nanoplates were formed accompanying with zincblende $CuInS_2$ QDs. A higher OA dosage (2~3 mL) led to the production of wurtzite $CuInS_2$ hexagonal nanoplates. The formation of the $CuInS_2$ nanocrystals with tunable structures was mainly attributed to the role of OA dosage in the formation and transformation of a $CuIn(SR)_x$ intermediate. A high OA dosage could facilitate the formation and crystallization of the intermediate, giving a metastable wurtzite $CuInS_2$ structure which can be gradually converted into stable zincblende $CuInS_2$ QDs as the reaction proceeded. But a low OA dosage would lead to a low crystallinity of the intermediate, and thus transformation into zincblende $CuInS_2$ phase easily. Therefore, our work could provide guidance for the controllable synthesis of other multi-component chalcogenide nanocrystals.

Introduction

At present, colloidal semiconductor nanocrystals have attracted much scientific attention due to their size and shape dependent properties and applications in the various fields.[1-3] As a typical ternary chalcogenide material, $CuInS_2$ is a I-III-VI_2 direct semiconductor with a bulk band gap of 1.45 eV, high extinction coefficient in the visible spectral range, exceptional radiation hardness and low toxicity.[4-6] Therefore, $CuInS_2$ has been the focus of much recent research, and are widely used as light-emitting and solar-harvesting materials.[7-9] $CuInS_2$ has three crystal structures: chalcopyrite, zincblende and wurtzite.[10,11] Chalcopyrite $CuInS_2$ is thermodynamically favored at room temperature whereas the zincblende and wurtzite structures are stable only at high temperatures. In the zincblende and wurtzite structures, the indium and copper atoms are randomly distributed over the cation sites of the lattice,[12,13] which allows a flexibility of stoichiometry and thus tunes the Fermi energy over a wide range. Due to the difference in the three structures, $CuInS_2$ nanocrystals will exhibit different optical properties by controlling their phase structure.

Recently, the most common synthesis methods of $CuInS_2$ nanocrystals include solvothermal method,[14,15] hot-injection method[16,17] and heat-up method.[18,19] Pan et al. first reported $CuInS_2$ nanocrystals with the zincblende and wurtzite structure by using dodecanethiol and OA as capping agent, respectively.[20] In particular, Liu et al. found that $CuInS_2$ nanoplates with wurtzite-zincblende polytypism could be synthesized by one-pot thermolysis of a mixture solution of metal chlorides, 1-dodecanethiol and OA in 1-octadecene. [21] They also prepared zincblende nanoparticles and wurtzite nanoplates by simply altering the dosage of 1-dodecanethiol. In the above reports, OA is usually used as a surfactant to avoid the aggregation of nanocrystals[21,22] or as a capping agent to synthesize $CuInS_2$ nanocrystals with a certain phase.[23,20,24] As is known, OA can affect the decomposition rate of metal precursors,[25,26] and thus put important effects on the nucleation rate of $CuInS_2$ nanocrystals which can determine the phase of nuclei.[10] In this sense, the phase structure of $CuInS_2$ nanocrystals will be affected by OA dosage. However, there have been no reports so far that the phase structure of $CuInS_2$ nanocrystals can be tuned by varying the OA dosage. This is probably because the phase selectivity mechanism of $CuInS_2$ nanocrystals is still unclear. Therefore, it is of great significance to investigate the phase selectivity mechanism in detail.

Herein, $CuInS_2$ nanocrystals with tunable structures were synthesized by a facile heat-up method through altering the OA dosage. Zincblende QDs with a triangular pyramid shape were synthesized at a low OA dosage (< 1 mL) while a mixture of zincblende $CuInS_2$ QDs and wurtzite $CuInS_2$ nanoplates were formed at a moderate OA dosage (~1.5 mL). When a high OA

dosage (2~3 mL) was used, wurtzite nanoplates were obtained but a few wurtzite nanoplates would be dissolved to form zincblende QDs as the reaction continued. Moreover, an OA assisted formation mechanism was proposed and discussed in detail for the production of $CuInS_2$ nanocrystals with tunable structures. Finally, the optical properties of as-prepared $CuInS_2$ nanocrystals were also investigated.

Experimental

Materials

All chemicals were used as received without further purification. Copper (I) chloride (CuCl, > 97.0%), indium (III) chloride tetrahydrate ($InCl_3 \cdot 4H_2O$, 99.99%), 1-dodecanethiol (DDT), oleic acid (OA), n-hexane, toluene, acetone were purchased from Sinopharm Chemical Reagent Co., Ltd and 1-octadecene (ODE, 90%) was purchased from Aladdin.

Synthesis of $CuInS_2$ nanocrystals

In a typical synthesis, 0.8 mmol CuCl, 0.8 mmol $InCl_3 \cdot 4H_2O$, 2 mL DDT, x mL OA (x = 0, 1, 1.5, 2, 3) and (10-x) mL ODE were added to a 50 mL three-necked flask. The reaction mixture was degassed at 100 °C for 30 min. After that, the solution was heated to 200 °C under argon flow and kept there for 30 min. The obtained solution was cooled down to room temperature and precipitated by acetone, then isolated by centrifugation and the supernatant liquid was decanted. And, the isolated solid was dispersed in hexane. The above centrifugation and isolation procedure was the repeated several times for purification of the prepared $CuInS_2$ NCs. Finally, the products were redispersed in toluene or dried in the air at 80 °C under vacuum for further analyses.

Characterizations

The powder X-ray diffraction (XRD) measurements were performed using a D8 Advance X'Pert Pro X-ray diffractometer. Transmission electron microscope (TEM) and high resolution transmission electron microscope (HRTEM) images were taken with a JEM 2100F microscope operated at 200 kV. Selected area electron diffraction (SAED) patterns and energy dispersed X-ray spectra (EDX) were performed on the same microscope. X-ray photoelectron spectra (XPS) were recorded on an AXIS-ULTRA DLD-600W X-ray photoelectron spectrometer. Fourier transform infrared spectra (FT-IR) were recorded on a Lambda 750S spectrometer. The as-prepared $CuInS_2$ nanocrystals were dispersed in hexane and the optical absorption spectra were measured using a Shimadzu UV-1601 UV-vis spectrometer with pure toluene as the reference. At first, the pure hexane was added into a cuvette to take a baseline, and then the $CuInS_2$ nanocrystals were dispersed in hexane into the cuvette for the UV-vis adsorption spectra.

Results and discussion

Synthesis and characterization of $CuInS_2$ nanocrystals

$CuInS_2$ (CIS) nanocrystals (NCs) were prepared by a heat-up method from 0.8 mmol CuCl, 0.8 mmol $InCl_3 \cdot 4H_2O$ and 2 mL DDT in noncoordinating solvent ODE with different dosages of OA. The XRD patterns of typical products synthesized using different OA dosages are shown in Fig. 1. The products prepared using low OA dosages (0 mL and 1 mL) are zincblende CIS while a wurtzite phase is obtained using higher OA dosages (2 mL and 3 mL). Moreover, a mixture of wurtzite and zincblende CIS is synthesized when the volume of OA is 1.5 mL. The difference between chalcopyrite phase and zincblende phase is very small, but the CIS NCs with zincblende phase usually have a diffraction peak of (200).[20,26] And the absence of the (101), (103) and (211) reflection peaks of chalcopyrite structure can be an evidence for the zincblende structure.[21,24] Compared with the simulated diffraction patterns,[21,27] all the peaks marked in the XRD patterns of CIS nanocrystals match well. The typical TEM, HRTEM and SAED images of CIS nanocrystals obtained with different OA dosages are shown in Fig. 2. Triangular pyramid nanoparticles are observed in the samples synthesized using 1 mL OA (Fig. 2a) and the size of these triangular pyramids is around 6 nm, which is twice smaller than the exciton radius of CIS (4.1 nm).[23] Thus, the zincblende nanocrystals with a triangular pyramid shape can be called as QDs. Both triangular pyramids QDs and hexagonal nanoplates synthesized using 1.5 mL OA can be observed in Fig. 2b. The size of these triangular pyramid QDs is around 5 nm and the diameter of nanoplates is 80-200 nm. Fig. 2c exhibits the hexagonal nanoplates obtained using 2 mL OA. The nanoplates have a diameter of *ca.* 200 nm, which is much larger than the size of QDs. This will be discussed in detail later.

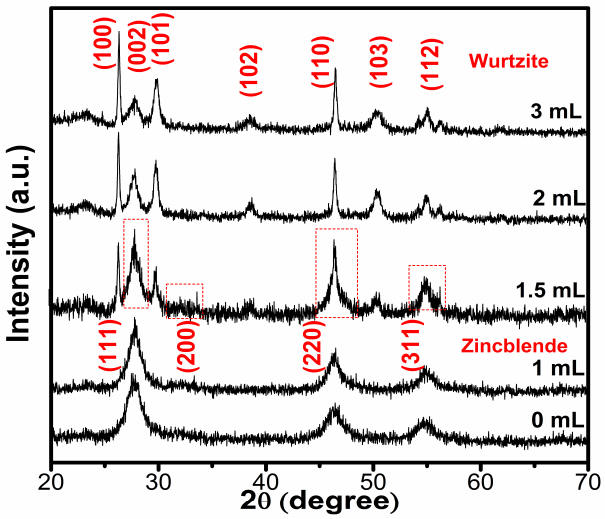

Fig. 1 XRD patterns of typical products synthesized using different OA dosages at 200 °C for 30 min: 0 mL, 1 mL, 1.5 mL, 2 mL, 3 mL.

The crystalline nature of the CIS NCs can be further revealed by using HRTEM and SAED characterizations. Fig. 2d shows HRTEM image of CIS triangular pyramids obtained using 1 mL OA. It can be observed that all the distances of the lattice fringes are 0.32 nm, which is in good agreement with the distance between the (111) planes of zincblende phase. In addition, if the CIS pyramids are of zincblende phase, then the four facets should be (111) face,[26,28] which is also consistent with the observation. Therefore, the CIS pyramids are of the zincblende phase exposed with (111) planes. The corresponding

SAED pattern is shown in Fig. 2g, and the ring pattern can be indexed to the (111), (220), (311), (400), (331) and (422) of zincblende phase. Fig. 2e exhibits HRTEM image of CIS triangular pyramids and hexagonal nanoplates synthesized using 1.5 mL OA. It is clear that the lattice fringes of the nanoplate with a distance of 0.34 nm correspond to (100) planes of wurtzite CIS, and the lattice fringes of the triangular pyramids with a distance of 0.32 nm are consistent with (111) planes of zincblende CIS. So both zincblende phase and wurtzite phase are contained in the sample synthesized using 1.5 mL OA, which accords with the above XRD result. Fig. 2f shows HRTEM image of CIS nanoplate obtained using 2 mL OA. The clear lattice fringes with a distance of 0.34 nm are consistent with (100) planes of wurtzite CIS. The SAED pattern (Fig. 2i) of the corresponding nanoplate reveals well single-crystalline nature of a nanoplate.

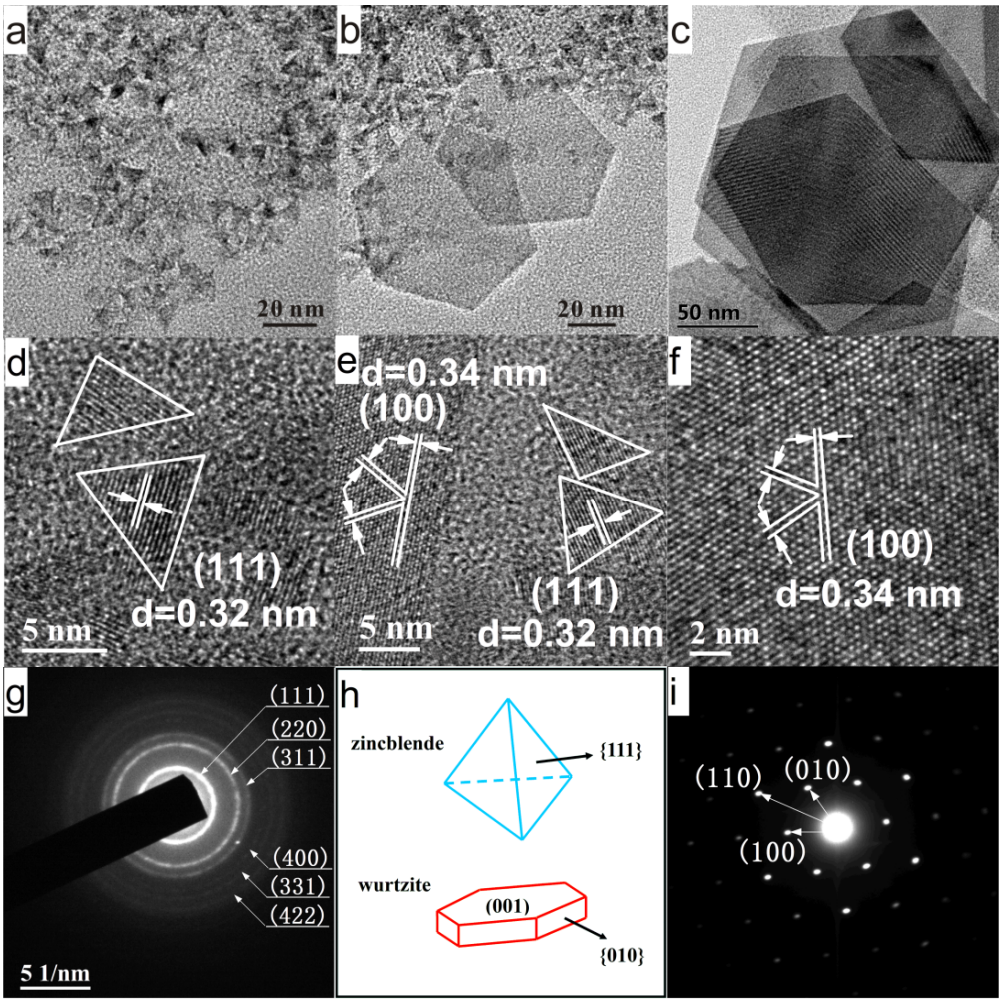

Fig. 2 (a and d) TEM, HRTEM images and (g) SAED pattern of zincblende CIS QDs synthesized using 1 mL OA; (b, e) TEM and HRTEM images of wurtzite and zincblende CIS mixture obtained using 1.5 mL OA; (c, f) TEM, HRTEM images and (i) SAED pattern of wurtzite CIS nanoplates synthesized using 2 mL OA; (h) the models of CIS triangular pyramid nanoparticles and hexagonal nanoplates.

The valence states and composition of the as prepared $CuInS_2$ nanocrystals were determined from XPS measurements. Two typical XPS spectra of pyramid nanoparticles and nanoplates are similar in Fig. 3. The full spectra in Fig. 3a show the presence of Cu 2p, In 3d and S 2p peaks, confirming the existence of these elements in the two samples. The binding energies of Cu $2p_{3/2}$ and Cu $2p_{1/2}$ are located at 932.5 eV and 952.3 eV with a peak splitting of 19.8 eV (Fig. 3b), in agreement with the reported values for Cu^+.[21] In addition, the copper Auger parameter is 1849.2 eV; it was calculated from the sum of the binding energy of the $2p_{3/2}$ XPS peak and the kinetic energy (KE) of the $L_3M_{45}M_{45}$ Auger peak (at 916.7 eV). Thus, copper oxidation state is thus +1 in the both samples.[13] The In 3d peaks were located at 444.8 eV and 452.3 eV with a peak splitting of 7.5 eV (Fig. 3c), corresponding to In^{3+}. In addition, the indium $M_4N_{45}N_{45}$ Auger peak at 407. 2 eV gives an Auger parameter of 852.0 eV, which suggests that the oxidation state of indium in the $CuInS_2$ samples is +3. The S 2p peaks at 161.7 eV and 162.8 eV with a peak splitting of 1.1 eV in Fig. 3d match well with S^{2-}. Through quantification of peaks, the molar ratios of Cu : In : S of pyramid nanoparticles and nanoplates are 1.30 : 1 : 1.95, and 1.61 : 1 : 2.46, respectively. Due to the large size of nanoplates, the above composition (Cu : In : S = 1.61 : 1 : 2.46) calculated from XPS result is probably

the elemental surface composition of $CuInS_2$ nanoplates, and thus deviates largely from the stoichiometric ratio. Therefore, EDX characterization was carried out and the result in Fig. S2 gives a Cu : In : S ratio of 1.30 : 1 : 1.83 for $CuInS_2$ nanoplates. It can be seen that, the both as-prepared samples are copper-rich with respect to the stoichiometric $CuInS_2$.

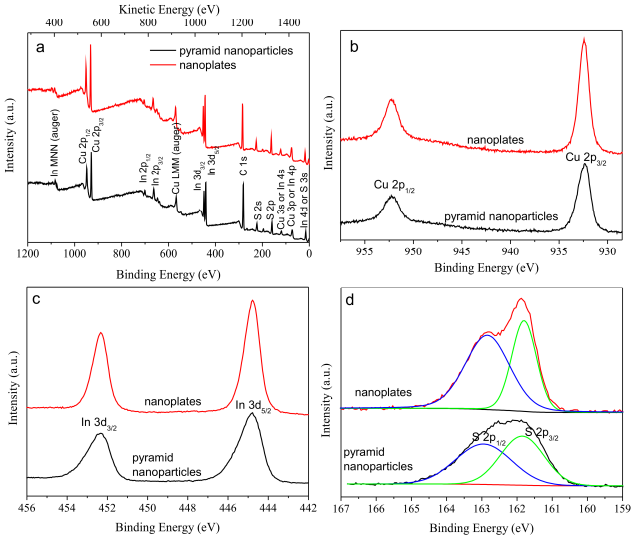

Fig. 3 XPS spectra of the pyramid nanoparticles and nanoplates: (a) survey spectrum, (b) Cu 2p, (c) In 3d, and (d) S 2p.

Formation mechanism of $CuInS_2$ nanocrystals

To investigate the effect of OA dosage on the CIS structures, the reaction process was observed and several samples were prepared. In our reaction system, CuCl, $InCl_3 \cdot 4H_2O$ were used as copper source and indium source, and DDT was used as sulfur source and surfactant. ODE was non-coordinating solvent and OA was served as co-capping agent. The OA dosage was tuned from 0 mL to 3 mL, and the total volume of OA and ODE was kept at 10 mL while the volume of DDT was fixed at 2 mL. It is said that DDT can easily react with certain metal salts, producing metal thiolates.[23] In our reaction system, when CuCl, $InCl_3 \cdot 4H_2O$, DDT, ODE and OA were mixed together at room temperature, a turbid white liquid containing metal thiolates were obtained. The metal thiolates were solved gradually during the heating process. When the temperature was kept at 100 °C, a clear solution was formed. It is interesting to note that the colours of the clear solutions are light yellow, yellow, brown and brown at the OA dosage of 0 mL, 1 mL, 2 mL, 3 mL, respectively, as shown in Fig. 4a. This is probably attributed to the state of intermediates affected by OA dosage. Then the clear solutions were heated to 200 °C gradually, and the colour of the solution began to change at 190 °C. At 0 mL OA, the colour of the clear solution is gradually turned from light yellow to brown and to dark brown as the reaction proceeds. At 1 mL and 1.5 mL OA, the colour is varied from yellow to brown and to dark brown. At 2 mL and 3 mL OA, the colour is turned from brown and to dark brown. The colour variation implies that intermediate compounds are formed by metal ions and DDT, and then these intermediates decomposed into CIS nanocrystals.[9,22] Therefore, it is considered that the OA dosage affects the initial state of the intermediates and nucleation of CIS nanocrystals.

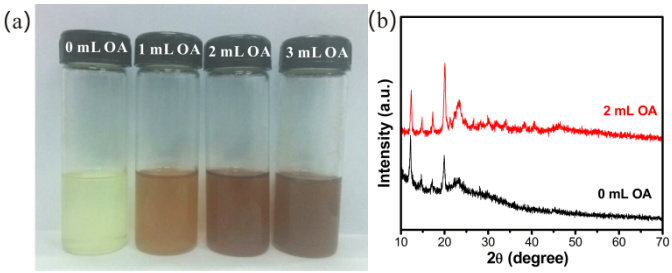

Fig. 4 (a) Photographs of clear solution formed at 100 °C with different OA dosages, and (b) XRD patterns of the intermediates prepared with 0 mL and 2 mL OA, respectively.

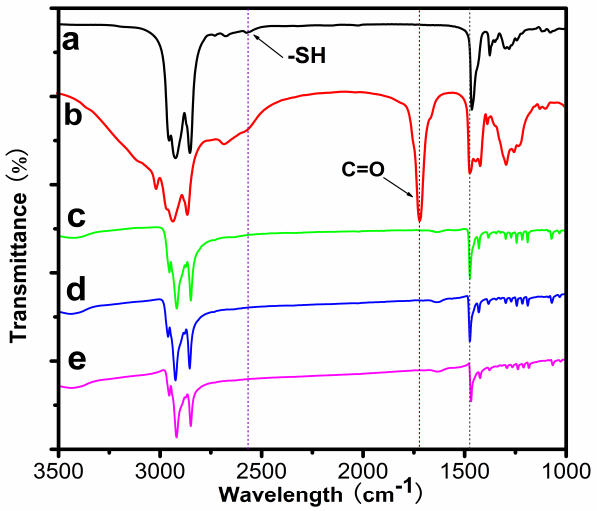

Fig. 5 FT-IR spectra of (a) pure DDT; (b) pure OA; (c) intermediate prepared at 100 °C; (d) CIS NCs and intermediate prepared at 190 °C; (e) CIS NCs prepared at 200 °C for 30 min.

To determine the composition of the intermediates, XRD and FTIR characterizations were carried out for the samples taken out from reaction solution with 0 mL and 2 mL OA, respectively. As show in Fig. 4b, all the diffraction peaks match well with the XRD pattern of $CuIn(SR)_x$ complex, as suggested in the previous reports.[21,24] XRD peak positions of the two intermediates are similar, while the intensities of low-angle peaks for the intermediates with 2 mL OA are much stronger than that without OA. In addition, there are more diffraction peaks for the intermediates with 2 mL OA than that without OA. This indicates that $CuIn(SR)_x$ complex is more stable in the mixture of OA and ODE than only in ODE. That is, high OA dosage can promote the formation and crystallization of $CuIn(SR)_x$ complex. To verify the intermediate formed, FT-IR spectra were measured for pure DDT, pure OA, pure intermediate, mixture of intermediate and $CuInS_2$ nanocrystals, and pure $CuInS_2$ nanocrystals, respectively (Fig. 5). It is shown that all samples have bands at 2925 and 2854 cm^{-1}, which is attributed to the C-H stretching vibration.[24] Compared with

pure DDT and OA, the absence of the S-H vibration at 2572 cm^{-1} and C=O vibration mode around 1550~1700 cm^{-1} for the imetrmediate and $CuInS_2$ nanocrystals indicates that the formation of metal-sulfide bonds in these compounds does occur, and there are no metal oleates in the intermediate.[26]

The formation and crystallization of $CuIn(SR)_x$ complex promoted by a high OA dosage can be explained by the Hard–Soft-Acid-Base (HSAB) principle.[29] As is known, Cu^+ and In^{3+} are soft and hard acids, respectively, and DDT is a soft base.[23] Usually, a soft acid tends to bind preferentially with a soft base rather than a hard base.[26] In this sense, DDT can coordinate well with Cu^+ but cannot bind tightly with In^{3+} and thus it is difficult to form stable $CuIn(SR)_x$ complex without OA or with low OA dosage. However, at high OA dosage, OA as a hard base can collaborate with DDT offering suitable coordination with In^{3+} to produce stable $CuIn(SR)_x$ complex. This is in good agreement with the above results. According to the previous report,[24] stable $CuIn(SR)_x$ complex as intermediates will lead to the formation of wurtzite CIS nanocrystals while unstable intermediates will be favourable for the production of zincblende CIS nanocrystals. In this sense, a high OA dosage will finally result in the formation of wurtzite CIS nanocrystals.

To further understand the growth mechanism of CIS NCs with different structures, CIS NCs synthesized using 0 mL and 2 mL OA at 200 °C at different reaction times were characterized by XRD. As shown in Fig. 6a, the XRD pattern of the sample taken out at the initial stage of nucleation (190 °C) is consisted of the diffraction peaks of zincblende CIS and $CuIn(SR)_x$ complex (as shown in Fig. 4b). The sample contains both zincblende CIS NCs and $CuIn(SR)_x$ complex. It can be found that, when the reaction time is prolonged, the diffraction peak intensity of zincblende CIS is increased while that of $CuIn(SR)_x$ complex decreases. At 60 min, the $CuIn(SR)_x$ complex probably has completely converted into zincblende CIS due to their diffraction peak disappears. This indicates that $CuIn(SR)_x$ complex is formed at first and then decomposed into zincblende CIS nuclei. The XRD pattern of the sample obtained at the initial stage of nucleation (190 °C) with 2 mL OA is presented in Fig. 6b. It can be found that the sample is consisted of wurtzite CIS and $CuIn(SR)_x$ complex. But the content of wurtzite CIS is very small due to the relative low intensity of diffraction peaks. As the reaction continues, the $CuIn(SR)_x$ complex is decomposed gradually and more wurtzite CIS is obtained (seen in Fig. 6b). However, the zincblende phase CIS emerges at 60 min and 90 min. From the TEM images (as shown in Fig. S1), it can be observed that a part of wurtzite nanoplates is dissolved to form new zincblende nanoparticles because the zincblende CIS is thermodynamically more stable than the wurtzite CIS.[12]

As seen in Fig. 6, the relative intensity of diffraction peaks for $CuIn(SR)_x$ complex using 2 mL OA was stronger than that without OA at the same reaction time, indicating that the formed $CuIn(SR)_x$ complex is more stable in the reaction solution with 2 mL OA than that without OA. That is to say, the decomposition rate of $CuIn(SR)_x$ in the solution without OA is faster than that with 2 mL OA. When the $CuIn(SR)_x$ complex is comparatively stable, the low decomposition rate will lead to the formation of a few metastable wurtzite $CuInS_2$ nuclei. In addition, OA is also used as a surfactant and its capping ligands is selectively absorbed on the (002) facet of wurtzite CIS nuclei with higher surface energy, so the growth of (002) facet is inhibited and finally large nanoplates are produced. Conversely, When the $CuIn(SR)_x$ complex has a low crystallinity, the high decomposition rate can result in the large amounts of zincblende nuclei.[10] But the growth rate of zincblende phase is slower than that of wurtzite phase due to the difference in the concentration of growth solution. This is because the production of zincblende nuclei can consume more metal ions in the reaction solution. Therefore, the size of zincblende CIS nanoparticles is small while wurtzite CIS nanoplates have large size.

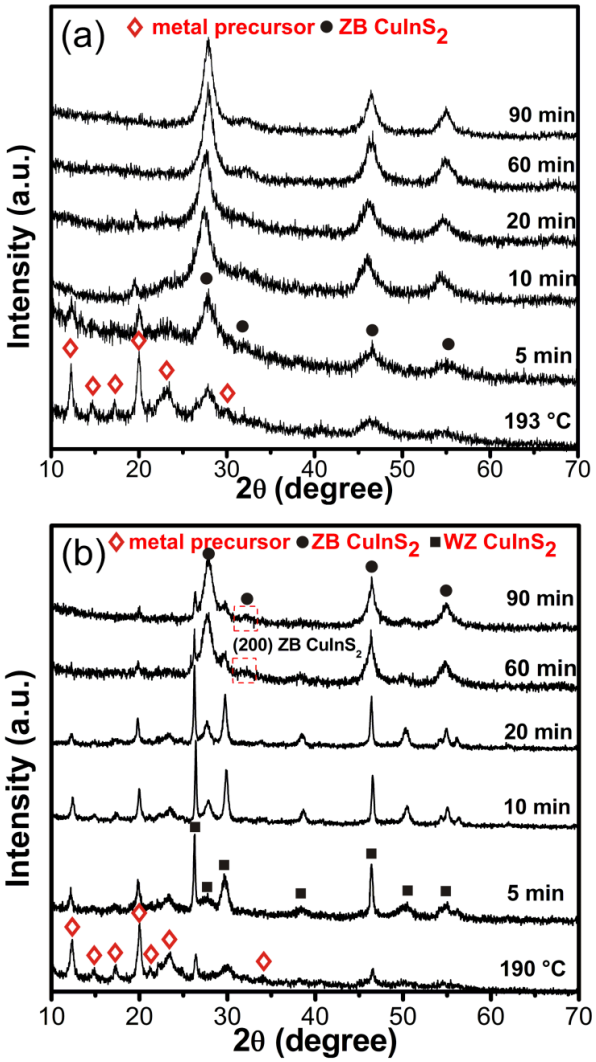

Fig. 6 XRD patterns of CIS NCs taken out from the reaction solution with OA (a) 0 mL and (b) 2 mL OA at different times: 5 min, 10 min, 20 min, 60 min, 90 min at 200 °C; 190 °C was the initial stage of nucleation of CIS NCs.

Base on the above experimental analysis, the illustration for the growth mechanism of zincblende and wurtzite CIS NCs formation is presented in Scheme 1. It can be considered that

the state of $CuIn(SR)_x$ complex and nucleation rate of CIS NCs play a crucial role in determining whether the phase of CIS nuclei is zincblende or wurtzite. At a low OA dosage, the coordination of DDT and In^{3+} is weak, the formed $CuIn(SR)_x$ complex is not stable. In this sense, the $CuIn(SR)_x$ complex is easy to decompose and thus the nucleation rate is fast, resulting in a large amount of zincblende CIS nuclei. Because most of the metal monomers are consumed, the growth rate is slow and thus zincblende (ZB) CIS nanoparticles with small size are formed finally. On the contrary, when the OA dosage is high, OA can collaborate with DDT offering suitable coordination with In^{3+} to produce relatively stable $CuIn(SR)_x$ complex. And thus, the metal thiolates are difficult to decompose and the nucleation rate is slow, resulting in a small amount of wurtzite (WZ) CIS nuclei. The concentration of the metal monomers is high in the reaction solution, so the growth rate is fast and wurtzite CIS nanoplates with large size are synthesized. As the reaction continues, the obtained wurtzite nanoplates begin to be dissolved and new zincblende nanoparticles are generated. At a moderate dosage of OA, the nucleation rate and growth rate are moderate, producing both zincblende nanoparticles and wurtzite nanoplates.

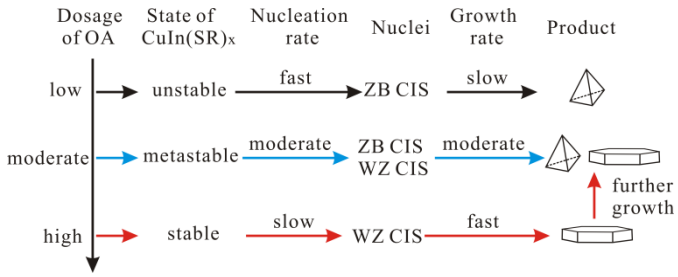

Scheme 1 Schematic formation mechanism of CIS nanocrystals using different OA dosages.

Optical properties of CIS nanocrystals

Optical properties of colloidal nanocrystals are of great importance for their potential applications as optoelectronic materials. It has been known that the optical properties of ternary NCs depend on their size, shape, composition, phase structure and surface states.[22] The UV-vis absorption spectra of the as-prepared CIS NCs have been measured at room temperature and are shown in Fig. 7. It can be observed that there is a broad absorption in the visible region with a tail in the long-wavelength direction. And the absorption band moves to a longer wavelength as the volume of OA is increased from 1 mL to 2 mL. For the direct band gap semiconductor, the band gap can be determined by extrapolation from the linear region of a plot of $(\alpha hv)^2$ *vs.* hv (α=absorption coefficient, h = Plank' s constant and v = frequency),[24,30] by which it is estimated that the band gap of CIS NCs synthesized using 1 mL , 1.5 mL and 2 mL OA are 1.71 eV, 1.55 eV and 1.44 eV, respectively. It is reported that zincblende $CuInS_2$ has a band gap of 1.07 eV,[23] which is much smaller than the experimental result 1.71 eV. This is because the zincblende $CuInS_2$ nanoparticles have a smaller size of *ca.* 6 nm with respect to the excition radius of CIS.[23] The band gap of wurtzite $CuInS_2$ nanoplates with a large size is 1.44 eV, corresponding to the reported result.[21,24] The CIS NCs synthesized using 1.5 mL OA have a band gap of 1.55eV, which is attributed to the combination of zincblende CIS and wurtzite CIS.

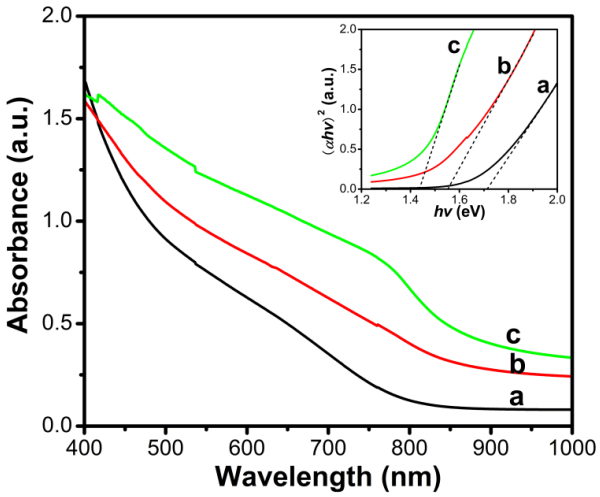

Fig. 7 Room temperature UV-vis absorption spectra of as-prepared CIS nanacrystals with zincblende (a), mixture of zincblende and wurtzite (b), wurtzite (c) structures; inset shows the plot of $(\alpha hv)^2$ *vs.* hv, indicating the optical gap of 1.44 eV, 1.55 eV and 1.71 eV for the corresponding samples.

Conclusions

In conclusion, zincblende and wurtzite $CuInS_2$ nanocrystals were synthesized by a simple thermolysis of CuCl, $InCl_3 \cdot 4H_2O$ and DDT precursors in a non-coordinating solvent ODE with adjusting the OA dosage. OA plays a crucial role in the nucleation rate of CIS and puts important impacts on the structures of CIS nanocrystals. Zincblende $CuInS_2$ nanoparticles could be obtained at a low dosage of OA (< 1 mL) while a mixture of zincblende $CuInS_2$ nanoparticles and wurtzite $CuInS_2$ nanoplates formed at a moderate dosage of OA (~1.5 mL). When the OA dosage was high (2~3 mL), wurtzite $CuInS_2$ nanoplates were produced but a part of them would be dissolved and transformed into new zincblende nanoparticles as the reaction proceeded. By studying the growth mechanism of $CuInS_2$ nanocrystals with different phase structures in detail, we suggest that the state of $CuIn(SR)_x$ complex and nucleation rate of CIS NCs can determine the phase structure of NCs. The $CuIn(SR)_x$ complex is unstable and the nucleation rate is fast, resulting in zincblende CIS QDs. When $CuIn(SR)_x$ complex is relatively stable and the nucleation rate is slow, wurtzite CIS nanoplates with larger size were obtained. More importantly, OA can help DDT coordinate with metal cations to form stable $CuIn(SR)_x$ complex as intermediates, thus reducing the decomposition rate of intermediates and then slowing down the nucleation rate of $CuInS_2$. Our work will make a contribution to the control synthesis of other multi-component chalcogenide nanocrystals.

Acknowledgements

This work was supported by the Doctoral Foundation of Ministry of Education Priority Development Projects (No. 20130143130002), National Natural Science Foundation of China (No. 51032005), Open Foundation of the State Key Laboratory of Silicate Materials for Architectures at WUT (No. SYSJJ2013-06), the fundamental Research Funds for the Central Universities (WUT: 2014-IV-012) and the China Postdoctoral Science Foundation (No. 2014M552097). We also thanked Dr. Qingwu Huang at the Analytic Testing Center in Huazhong University of Science and Technology for XPS measurement. And the technology was supported by Analytic Testing Center of WUT for carrying out XRD, FTIR and TEM analysis.

Notes and references

State Key Laboratory of Silicate Materials for Architectures, Wuhan University of Technology (WUT), No. 122, Luoshi Road, Wuhan 430070, P. R. China. *Corresponding author. Tel.: +86-027-87652553; Fax: +86-027-87883743. E-mail address: tiansq@whut.edu.cn (S. Tian), opluse@whut.edu.cn (X. Zhao).

Electronic Supplementary Information (ESI) available: TEM and HRTEM images of CIS nanoparticles synthesized using 2 mL OA at 200 °C for 60 min. See DOI: 10.1039/b000000x/

1 C. B. Murray, C. R. Kagan and M. G. Bawendi, Annu. Rev. Mater. Sci., 2000, **30**, 545-610.
2 Y. N. Xia, P. D. Yang, Y. G. Sun, Y. Y. Wu, B. Mayers, B. Gates, Y. D. Yin, F. Kim and Y. Q. Yan, Adv. Mater., 2003, **15**, 353-389.
3 M. Law, J. Goldberger and P. D. Yang, Annu. Rev. Mater. Res., 2004, **34**, 83-122.
4 T. Pons, E. Pic, N. Lequeux, E. Cassette, L. Bezdetnaya, F. Guillemin, F. Marchal and B. Dubertret, ACS Nano, 2010, **4**, 2531-2538.
5 D. Wang, W. Zheng, C. Hao, Q. Peng and Y. Li, Chem. Commun., 2008, 2556-2558.
6 J. Kolny-Olesiak and H. Weller, ACS Appl. Mater. Interfaces, 2013, **5,** 12221-12237.
7 H. Z. Zhong, Z. L. Bai and B. S. Zou, J. Phys. Chem. Lett., 2012, **3**, 3167-3175.
8 L. Li, N. Coates and J. Moses, J. Am. Chem. Soc., 2009, **132**, 22-23.
9 D. Deng, Y. Chen, J. Cao, J. Tian, Z. Qian, S. Achilefu and Y. Gu, Chem. Mater., 2012, **24**, 3029-3037.
10 K. Nose, Y. Soma, T. Omata and S. Otsuka-Yao-Matsuo, Chem. Mater., 2009, **21**, 2607-2613.
11 M. Kruszynska, H. Borchert, J. Parisi and J. Kolny-Olesiak, J. Am. Chem. Soc., 2010, **132**, 15976-15986.
12 Y. Qi, Q. Liu, K. Tang, Z. Liang, Z. Ren and X. Liu, J. Phys. Chem. C, 2009, **113**, 3939-3944.
13 F. M. Courtel, R. W. Paynter, B. Marsan and M. Morin, Chem. Mater., 2009, **21**, 3752-3762.
14 T. L. Li and H. Teng, J. Mater. Chem., 2010, **20**, 3656-3664.
15 D. E. Nam, W. S. Song and H. Yang, J. Mater. Chem., 2011, **21**, 18220-18226.
16 X. Sheng, L. Wang, Y. Luo and D. Yang, Nanoscale Res. Lett., 2011, **6**, 562-572.
17 J. Niezgoda and M. Harrison, Chem. Mater. 2012, **24**, 3294-3298.
18 J. J. He, W. H. Zhou, J. Guo, M. Li and S. X. Wu, CrystEngComm, 2012, **14**, 3638-3644.
19 R. Yao, Z. Zhou, Z. Hou, X. Wang, W. Zhou and S. Wu, ACS Appl. Mater. Interfaces, 2013, **5**, 3143-3148.
20 D. Pan, L. An, Z. Sun, W. Hou, Y. Yang, Z. Yang and Y. Lu, J. Am. Chem. Soc., 2008, **130**, 5620-5621.
21 Z. Liu, L. Wang, Q. Hao, D. Wang, K. Tang, M. Zuo and Q. Yang, CrystEngComm, 2013, **15**, 7192-7198.
22 H. Zhong, Y. Zhou, M. Ye, Y. He, J. Ye, C. He, C. Yang and Y. Li, Chem. Mater., 2008, **20**, 6434-6443.
23 X. Lu, Z. Zhuang, Q. Peng and Y. Li, CrystEngComm, 2011, **13**, 4039-4045.
24 J. Chang and E. R. Waclawik, CrystEngComm, 2013, **15**, 5612-5619.
25 X. Wang, D. Pan, D. Weng, C. Y. Low, L. Rice, J. Han and Y. Lu, J. Phys. Chem. C, 2010, **114**, 17293-17297.
26 H. Zhong, S. S. Lo, T. Mirkovic, Y. Li, Y. Ding, Y. Li and G. D. Sholes, ACS Nano, 2010, **4**, 5253-5262.
27 N. Bao, X. Qiu, Y. A. Wang, Z. Zhou, X. Lu, C. A. Grines and A. Gupta. Chem. Commun., 2011, **47**, 9441-9443.
28 E. C. Greyson, J. E. Barton and T. W. Odom, Small, 2006, **2**, 368-371.
29 R. G. Pears, J. Am. Chem. Soc., 1963, **20**, 3533-3539.
30 V. M. Huxter, T. Mirkovic, P. S. Nair and G. D. Scholes, Adv. Mater., 2008, **20**, 2439-2443.

$CuInS_2$ nanocrystals with different phase structures were synthesized by a facile heat-up method through simply adjusting the OA dosage. This is because, a high OA dosage could facilitate the formation and crystallization of the $CuIn(SR)_x$ intermediate, giving metastable wurtzite $CuInS_2$ structure, while low OA dosage would lead to low crystallinity of the intermediate, and thus transformation into zincblende $CuInS_2$ phase.